JOURNAL OF HERPETOLOGY

The tadpole and karyotype of *Rhinella* (*Bufo*) *achavali* (Anura: Bufonidae)

FRANCISCO KOLENC[1,5], CLAUDIO BORTEIRO[1], LEONARDO COTICHELLI[2], DIEGO BALDO[2], CLAUDIO MARTÍNEZ DEBAT[3], AND FLORENCIA VERA CANDIOTI[4]

[1] *Sección Herpetología, Museo Nacional de Historia Natural, Montevideo, Uruguay*

[2] *Laboratorio de Genética Evolutiva, Instituto de Biología Subtropical (CONICET-UNaM), Facultad de Ciencias Exactas, Universidad Nacional de Misiones; Félix de Azara 1552, CPA N3300LQF. Posadas, Misiones, Argentina.*

[3] *Sección Bioquímica, Facultad de Ciencias, Universidad de la República, Montevideo, Uruguay*

[4] *CONICET - Fundación Miguel Lillo, San Miguel de Tucumán, Tucumán, Argentina*

[5] *Corresponding author. E-mail: fkolenc@gmail.com*

LRH: C. Borteiro et al.

RRH: Tadpole and karyotype of *Rhinella achavali*

ABSTRACT.— We describe the external morphology, buccal cavity, chondrocranium, hyobranchial skeleton and musculature of the tadpole of *R. achavali*, along with its karyotype. Tadpoles were found in a permanent streamlet, showing schooling behavior. External larval morphology seems to be much conserved in *Rhinella*, not helping in the characterization of the proposed species groups. Buccal cavity morphology confirms the distinctiveness of the *R. veraguensis* group with respect to other known *Rhinella*. Musculoskeletal characters show most features shared with other Bufonidae, except for some typical of the basal genus *Melanophryniscus*. Karyotype is composed of 22 biarmed chromosomes, with secondary constrictions in pair 7, like the other species in the *R. marina* group.

Key words: Ag-NOR; Buccal cavity; C-banding; Cytogenetics; Chondrocranium; Hyobranchial skeleton

The *Rhinella marina* species group was defined by Martin (1972, as the *Bufo marinus* group) on the basis of osteological characters. The species primarily included in this Neotropical group were large ones, usually reaching more than 10 cm of snout-vent length: *R. arenarum*, *R. icterica*, *R. marina*, *R. schneideri*, *R. poeppigii*, and *R. rubescens*. Some species subsequently included in the *R. marina* group were described in recent years: *R. achavali*, *R. cerradensis*, *R. jimi*, and *R. veredas* (Stevaux, 2002; Maneyro et al., 2004; Brandão et al., 2007; Maciel et al., 2007). A recent phylogenetic study confirmed the monophyly of this group (Maciel et al., 2010), although Vallinoto et al. (2010) found it to be paraphyletic, with the *R. crucifer* group nested within it. *Rhinella achavali* is native from hilly environments of Uruguay and southern Brazil and almost nothing is known about its biology (Maneyro et al., 2004; Kwet et al., 2006). According to Maciel et al. (2010), it is more closely related to *R. icterica*, *R. rubescens*, and *R. arenarum*.

Larval external morphology is known for most species in the *R. marina* group, except for *R. achavali*, *R. poeppigii*, and *R. veredas*. In contrast, little attention has been placed on the internal larval morphology, which has been studied only in *R. arenarum*, *R. marina*, and *R. schneideri* (Vera Candioti, 2007 and references therein). Cytogenetic studies were conducted on most species of this group (Kasahara et al., 1996; Azevedo et al., 2003; Amaro-Ghilardi et al., 2007), but the karyotype of *R. achavali* remains unknown.

In this work we describe the external morphology, buccal cavity, chondrocranium, hyobranchial skeleton and musculature of the tadpole of *R. achavali*, along with its karyotype. The results are compared with the available information about tadpole morphology and cytogenetics of *Rhinella*.

MATERIALS AND METHODS

Voucher specimens are stored at the herpetological collection of Museo Nacional de Historia Natural, Montevideo, Uruguay (MNHN). We collected tadpoles of *Rhinella achavali* at Curticeras, Departamento de Rivera, Uruguay, 31º00'S, 55º35'W, 200 m a.s.l., on 22 August 2008, euthanized with benzocaine, and then fixed them with formalin (10%). We identified the tadpoles by rearing some specimens through metamorphosis (voucher specimen MNHN 9467) and by DNA barcoding. For this purpose, we sequenced a fragment of 349 bp of the mitochondrial Cytochrome b gene from one tadpole from the same lot as those used in the description (MNHN 9468, GenBank KC567990, tissue sample taken from tail clip, stored in 95% ethanol) and from one specimen of *R. achavali* from Quebrada de los Cuervos, Departamento de Treinta y Tres, Uruguay (MNHN 9301, GenBank KC567989). The fragments were amplified using primers MVZ15 (Moritz et al., 1992) and H15149(H)

(Kocher et al., 1989) applying standard protocols, resolved on automated sequencers (Pasteur Institute, Montevideo, Uruguay), edited with Chromas Lite 2.1 (Technelysium) and aligned and compared with Mega 4.1 (Tamura et al., 2007). Sequences of the tadpole and of the reference specimen shared 99.4% identity. In addition, a BLAST search at GenBank resulted in a 100% identity of the tadpole sequence for a 52% overlap with a published sequence of *R. achavali* (GU178809.1, voucher specimen ZVCB 3801, paratype, Vallinoto et al., 2010).

Descriptions of tadpole external morphology were based on 10 specimens at stages 31−33 (Gosner, 1960), MNHN 9469 and 9470. The specimens were examined and measured to the nearest 0.1 mm using an ocular micrometer in a Nikon SMZ–10 stereoscopic microscope, except for total length which was measured with digital callipers. Twenty three morphometric variables were registered (Kolenc et al., 2009). Morphological terminology follows that of Altig and McDiarmid (1999a) and Lannoo (1987) for the lateral line system.

The buccopharyngeal cavities of five tadpoles (stages 31 and 33, MNHN 9471) were exposed and the structures stained with methylene blue for examination with stereomicroscope. One of them was prepared for scanning electron microscope examination of the oral disc and buccal cavity after Alcalde and Blotto (2006). Buccal terminology follows that of Wassersug (1976). Five larvae (stages 31 and 33, MNHN 9472) were stained for bone and cartilage examination after Taylor and Van Dyke (1985). To observe the musculature, tadpoles were colored with Lugol's solution before the enzymatic digestion step. Terminology follows that of Haas (2003).

Karyotypes were obtained from cell preparations of bone marrow tissue of three specimens captured at Curticeras, Rivera, on February 2006 (MNHN 9473–5). For methodology and terminology we follow Tomatis et al. (2009). Measurements throughout the text are given as mean ± SD.

RESULTS

Tadpole external morphology.—Tadpoles measure 29.7 ± 1.1 mm of total length. Body short (BL/TL = 0.44 ± 0.01), ovoid in dorsal view, depressed (BMH/ BMW = 0.81 ± 0.02), widest at the posterior portion of the abdominal region, and lower than the tail (TMH/BMH = 1.12 ± 0.05). Snout rounded in dorsal view, sloping in lateral view (Fig. 1A, B). Nostrils oval, dorsal (EN/ BWE = 0.33 ± 0.01), closer to the eyes than to the tip of the snout (FN/ END = 2.24 ± 0.35); marginal rim with a variably marked small, subtriangular, fleshy projection in medial margin. Eyes large (E/BWE = 0.19 ± 0.01) and lateral (EO/BWE = 0.62 ± 0.02). Pineal end organ not visible externally. Spiracle single, lateral, sinistral; spiracular tube entirely fused to the body wall, caudally projected. Spiracular opening oval, being its diameter smaller than the tube diameter, placed at the middle third of the body (RSD/BL = 0.68 ± 0.03). Neuromasts of angular, anterior oral, longitudinal oral, infraorbital, posterior infraorbital, supraorbital, posterior supraorbital, ventral, middle, dorsal, pregular, and postgular clusters noticeable. Vent tube medial, attached to the ventral fin. Tip of the tube reaching the free margin of the ventral fin. Tail long (TAL/TL = 0.63 ± 0.01) and straight. Maximum tail height at its first third. Dorsal fin originating at the body-tail junction, and both fins converging over its posterior half, ending rounded. Tail musculature not reaching the tail end; myomers evident with magnification.

Oral disc (Fig. 1C) anteroventral, medium sized (OD/BMW = 0.41 ± 0.02), and laterally emarginated. Marginal papillae arranged in a single row, with a wide dorsal gap (DG/OD = 0.80 ± 0.03) which is about twice the length of the ventral gap (VG/OD = 0.42 ± 0.05). Few to several submarginal papillae present laterally, in supraangular and infraangular regions. Jaw sheaths robust, pigmented distally and finely serrated, with free margin widely V-shaped in lower jaw and widely arch-shaped in upper one. Labial teeth with spatulate convex head, body and sheath clearly differentiated, the head bearing 11–18 marginal cusps (Fig. 2C). Labial tooth row formula 2(2)/3(1), being the gap in A2 larger than that of P1.

Measurements in mm: TL 29.7 ± 1.1, BL 11.0 ± 0.4, TMH 7.2 ± 0.4, BMW 8.0 ± 0.3, BWE 6.6 ± 0.3, BMH 6.5 ± 0.2, RSD 7.5 ± 0.3, FN 1.4 ± 0.1, END 0.6 ± 0.1, E 1.2 ± 0.1, EN 2.2 ± 0.1, EO 4.1 ± 0.1, OD 3.2 ± 0.2, DG 2.6 ± 0.2, VG 1.3 ± 0.1.

Coloration *in vivo*: body and tail musculature uniformly black, fins opalescent with scarce blood vessels. Coloration in formalin 10% after about two years of fixation slightly faded.

Buccopharyngeal cavity.— Buccal roof (Fig. 2A) with prenarial arena showing a short medial papilla, with or without scattered pustulations. Choanae large and almost transversely arranged; anterior margin with small prenarial papillae; narial valve thick and smooth. Inner surface of the choanae with ciliated epithelium in the anteromedial region (Fig. 2D). Postnarial arena with 3–6 pairs of conical postnarial papillae of unequal length, with pustulate tips; one or two pustulations just anterior to the median ridge. Median ridge triangular, high, wider at the base, with 2–4 irregular projections at the tip. Lateral ridge papillae well developed and three or more pustulate tips. Buccal roof arena delimited on both sides by 4–6 tall, conical papillae with tips usually bifurcate; numerous pustulations scattered among the papillae. Secretory pits arranged in a U-shaped display on the posterior margin. Dorsal velum short and with smooth margin, medially interrupted and with several oesophagic papillae at the middle region.

Buccal floor (Fig. 2B) with a pair of small, non-colored spurs directed anteromedially located posteriorly to the lower jaw sheath (Fig. 2E). Two infralabial papillae, tall, subcylindrical or compressed, bi-, tri-, or multifid with pustulate tips; they may or not overlap each other in the middle line. Four lingual papillae on the tongue anlage; tall, cylindrical, with pustulate tips or secondary branching, transversally aligned, all of similar length. In half the specimens, the lateral pair is bifurcated near the base. Prepocket region with some pustulations and up to 6 prepocket papillae on each side. Buccal pockets elongate and transversely arranged. Buccal floor arena delimited on both sides by 8–14 tall, conical papillae accompanied by numerous pustulations and small papillae. Ventral velum semicircular and supported by spicules; margin with small projections, more evident at the middle region; median notch absent. Secretory pits along the edge of the velum. Glottis not visible.

Chondrocranium.—Chondrocranium 47% of body length, rectangular (width/length = 0.84), dorsoventrally flattened, with greatest width at the level of the posterior part of the subocular bar (Fig. 3A). Suprarostral cartilage with single, U-shaped pars corporis and triangular partes alares with a well-developed posterior dorsal process (Fig. 3B). Adrostral cartilages absent. Nasal septum short and lamina orbitonasales triangular. Trabecular horns diverging from the ethmoid plate, long (25% of the total length of the chondrocranium), with a long (85% of the length) and narrow (32% of the free portion length) free portion, ventrally curve and almost uniformly wide. Anterior margin oblique and lateroventral margin, with lateral trabecular process. Cranial floor completely cartilaginous, with thin cartilage in the central area. Primary carotid and craniopalatine foramina visible. Notochordal canal evident in the posterior margin of the cranial floor. Lateral walls of the chondrocranium formed by the orbital cartilages. Optic foramen and oculomotor foramen visible on the posterior ends of the cartilage. Prootic foramen visible and almost opens dorsally because of the incomplete development of the taenia tecti marginalis. Chondrocranium open dorsally, and frontoparietal fenestra bordered on both sides by the taeniae tecti marginales and posteriorly by the tectum synoticum. Otic capsules ovoid, representing nearly 29% of the chondrocranium total length;

anterolateral processes small and rounded. Larval otic process absent. Operculum not yet developed. Otic capsules dorsally joined by the tectum synoticum.

Palatoquadrate long and relatively narrow, with a long, thin articular process, and a wide, dorsally rounded muscular process. Subocular bar with a smooth margin and rounded posterior region. Palatoquadrate attachment to the braincase via quadratocranial commissure, quadrato-orbital commissure, and ascending process. Quadratocranial commissure thin, bearing a well-developed, triangular quadratoethmoid process and a rounded antorbital process projecting dorsally. Quadrato-orbital commissure extending between the tip of the muscular process and the antorbital process. Pseudopterygoid process absent. Ascending process attachment ventral and posterior to the oculomotor foramen (low). Lower jaw composed by infrarostral and Meckel's cartilages (Fig. 3C). The latter sigmoid with dorsomedial and ventromedial processes, and articulating with the articular process of the palatoquadrate via a rounded retroarticular process. Infrarostral cartilages paired, short, rectangular and dorsally curved.

Ceratohyals (Fig. 3D) long with long, triangular anterior processes, acute, medially directed anterolateral processes, and wide posterior processes; articular condyle rounded and robust. Ceratohyals joined medially by the pars reuniens. Basihyal absent, and basibranchial long, bearing a short, quadrangular urobranchial process. Hypobranchial plates flat and triangular, and articulated medially leaving a posterior triangular gap. Ceratobranchials long, thin, and with lateral projections. Branchial processes I and II prominent. Ceratobranchials I and II continuous with the hypobranchial plates, distally joined by well-developed terminal commissures. Four cartilaginous spicules long and curve.

Musculature.—The cranial muscles of *R. achavali* tadpoles are shown in Figure 4 and their insertions described in Table 1.

Natural history.—Tadpoles of *Rhinella achavali* belong to the benthic ecomorphological guild, section II: A: 1 of McDiarmid and Altig (1999). They were found in a backwater section of a permanent streamlet, at a site of about 0.5 m depth, loosely grouped into a school close to the water surface, foraging between gramineous vegetation and filamentous algae.

Karyotype.—Diploid complement composed by 11 biarmed chromosome pairs, 2N = 2X = 22; fundamental number (FN) = 44 (Fig. 5). Six large pairs, one medium pair, and five small pairs of chromosomes. Pairs 1–3 and 5–7 were metacentric, whereas pair 4 was submetacentric. Interstitial secondary constrictions (SCs) present in pair 7. Centromeric relation (CR, expressed for each chromosome pair as percentage of the total complement) is detailed in Table 2. C-banding detected centromeric heterochromatic regions in all chromosomes, and also interstitially in the long arm of pair 3 and in the short arms of pair 7, adjacent to the SCs. Ag-NORs located interstitially in the short arms of chromosome pair 7, adjacent to the positive C-bands.

Discussion

The tadpoles of *Rhinella achavali* are similar to those of other species in the *R. marina* group already described: *R. arenarum* (Fernández, 1926; Cei, 1980; Echeverría and Fiorito de López, 1981; Vera Candioti, 2007), *R. cerradensis* (Maciel et al., 2007), *R. icterica* (Cei, 1980; Heyer et al., 1990), *R. jimi* (Mercês et al., 2009; Tolledo and Toledo, 2010), *R. marina* (Savage, 1960; Kenny, 1969), *R. rubescens* (Eterovick and Sazima, 1999) and *R. schneideri* (Cei, 1980; Rossa-Feres and Nomura, 2006). According to the available descriptions, the tadpoles of the *R. marina* group are very alike, and look like the typical pond-dwelling anuran larvae (for a comparative table, see Tolledo and Toledo, 2010). The *in vivo* coloration pattern in the different species is predominantly dark, uniformly dark brown or black; fins are scarcely pigmented. A remarkable feature of *R. cerradensis* is the spiracular tube lacking the external portion (Maciel et al., 2007). Neuromasts of the lateral line system were reported to date in *R. achavali* (present study), *R. arenarum* (Echeverría and Fiorito de López, 1981), illustrated to some extent in *R. cerradensis* by Maciel et al. (2007), but seem to have been overlooked in other descriptions. A visible pineal end organ was observed in tadpoles of some species of the bufonid genera *Rhinella* and *Melanophryniscus* (Baldo and Basso, 2004; Borteiro et al., 2006), but the remarkable pigmentation of the skin of the tadpoles of *R. achavali* does not allow its visualization. External larval morphology seems to be much conserved in *Rhinella*, not helping in the characterization of the proposed species groups.

In the oral disc, the ventral gap in the marginal papillae was proposed as a synapomorphy of Bufonidae (Haas, 2003), and is known to be absent only in *Rhinella scitula* and in the species of the genera *Ansonia*, *Leptophryne*, and *Werneria* (Altig and McDiarmid, 1999b; Caramaschi and Niemeyer, 2003). The generalized LTRF 2/3 is also present in all *Rhinella* tadpoles except for some species in the *R. granulosa* group (Borteiro et al., 2006). In tadpoles of the *R. marina* group, labial teeth are narrow-based, curved, and have a long, narrow head with 8–18 cusps along the entire margin of the head (Fiorito de López and Echeverría, 1989; Vera Candioti, 2007). Conversely, those species in the *R. granulosa* group having 2 lower labial tooth rows show shorter teeth with 2–5 long, broad, distal cusps (Echeverría, 1998; Vera Candioti and Altig, 2010).

Within the buccal cavity, *Rhinella achavali* tadpoles share with other congeneric species the prenarial ridge, two infralabial papillae, and four lingual papillae (Fabrezi and Vera, 1997; Echeverría, 1998; Vera Candioti, 2007). Only the buccal cavities of tadpoles of the *R. veraguensis* group have noticeable differences, including a poorly defined buccal roof arena, flap-like infralabial papillae, and 0–2 lingual papillae (Cadle and Altig, 1991; Aguayo et al., 2009). A pair of non-colored, anteromedially directed spurs are described in *R. achavali, R. arenarum* and *R. spinulosa* (Vera Candioti, 2007). Since the discussion by Wassersug (1980) about the spurs as buccal keratinized mouthparts, the definition of these structures has been broadened as to also include the pointed, non-colored projections within the buccal cavity of some *Scinax* species (Alcalde et al., 2011). The distribution of the character among *Rhinella* species needs to be reviewed in light of this interpretation.

The skeleton of *Rhinella* tadpoles described have several common features, such as a suprarostral with a single corpus and differentiated, dorsally fused alae, quadratoethmoid process and lateral process of trabecular horns present, and larval otic process absent (Fabrezi and Vera, 1997; Haas, 2003; Vera Candioti, 2007; Aguayo et al., 2009). The presence of a quadrato-orbital commissure is regarded as a synapomorphy of the clade joining all bufonids except *Melanophryniscus* (Frost et al., 2006). Likewise, the muscular system of *R. achavali* shows the two characters proposed as synapomorphies for Bufonidae by Haas (2003), i.e., the m. diaphragmatopraecordialis absent and the m. subarcualis rectus II–IV with a slip invading the branchial septum IV. Other common features include the m. mandibulolabialis composed of a single slip, the mm. levator mandibulae externus superficialis, l. m. e. profundus, and l. m. lateralis present, the m. subarcualis rectus I with three slips, the mm. levator arcuum branchialium IV and tympanopharyngeus not completely separated, and the m. interhyoideus posterior absent (Sedra, 1950; Carr and Altig, 1991; Haas, 2003; Vera Candioti, 2007; Aguayo et al., 2009).

The basic number of x = 11 chromosomes observed in *R. achavali* is generalized in Bufonidae, it was recorded in all analyzed genera (for review see Green and Sessions, 2007), with the exception of some species of *Amietophrynus* that has a derived basic number of 10 chromosomes (Bogart, 1968, 1972; Vitelli et al., 1982; Cunningham and Cherry, 2004). At present the 22 species of *Rhinella* that have been karyotyped exhibit 22 biarmed chromosomes (FN = 44), and although their karyotypes are very similar, the chromosome pairs bearing the SCs and Ag-NORs differ between species groups: pair 5 in the *R. granulosa* group, pairs 7 or 11 in the *R. spinulosa* group, pair 10 in the *R. margaritifera* and *R. veraguensis* groups, and pair 7 in the *R. marina* and *R. crucifer* groups (Baldissera et al., 1999; Amaro-Ghilardi et al., 2007, and references therein). As observed in other species of the *R. marina* group (Kasahara et al., 1996; Azevedo et al., 2003; Amaro-Ghilardi et al., 2007), the karyotype of *R. achavali* presents small C-bands in the centromeric and pericentromeric regions of all chromosomes, which account for an apparently very conservative pattern of constitutive heterochromatin distribution in the *R. marina* group.

The occurrence of tadpole aggregative behaviour seems to be common in the *Rhinella marina* group: it is exhibited by *R. achavali* (present study), *R. marina* (Kenny, 1969), *R. rubescens* (Eterovick and Sazima, 1999), and it was observed by us in *R. arenarum* and *R. schneideri* from Uruguay and Argentina (unpubl. data). The formation of these loose and weakly polarized tadpole aggregations fits into the schooling behaviour Type I of Caldwell (1989), and is probably characteristic of all species in the *R. marina* group and of the related *R. crucifer* group, since it was reported in *R. crucifer* (Eterovick, 2000) and *R. pombali* (Lourenço et al., 2010). This character is also present in other Bufonidae not closely related to *Rhinella* (e.g., Beiswenger, 1977; Breden et al., 1982; Eluvathingal et al., 2009).

Acknowledgments.—We thank J.E. García, J. Valbuena, and G. Duarte, who kindly assisted during fieldwork. DINARA-MGAP and the Service of Electron Microscopy of the Faculty of Sciences, Universidad de la República, gave logistic support. CB and FK received partial financial support from ANII/SNI. Collection permits # 417/03, 195/06, and 18/09 were extended by División Fauna/MGAP- Uruguay.

LITERATURE CITED

Aguayo, R., E.O. Lavilla, M.F. Vera Candioti, and T. Camacho. 2009. Living in fast-flowing water: morphology of the gastromyzophorous tadpole of the bufonid *Rhinella quechua* (*R. veraguensis* group). Journal of Morphology 270:1431–1442.

Alcalde, L., and B.L. Blotto. 2006. Chondrocranium, cranial muscles and buccopharyngeal morphology on tadpoles of the controversial leptodactylid frog *Limnomedusa macroglossa* (Anura: Leptodactylidae). Amphibia-Reptilia 27:241−253.

Alcalde, L., F. Vera Candioti, F. Kolenc, C. Borteiro, and D. Baldo. 2011. Cranial anatomy of tadpoles of five species of *Scinax* (Hylidae, Hylinae). Zootaxa 2787:19-36.

Altig, R. and McDiarmid, R.W. 1999a. Body plan. Development and morphology. Pp. 24–51 in R.W. McDiarmid and R. Altig (Eds.), Tadpoles: The Biology of Anuran Larvae. University of Chicago Press, USA.

Altig, R. and McDiarmid, R.W. 1999b. Diversity. Familial and generic characterizations. Pp. 295–337 in R.W. McDiarmid and R. Altig (Eds.), Tadpoles: The Biology of Anuran Larvae. University of Chicago Press, USA.

Amaro-Ghilardi, R.C., M.J. de Jesus Silva, M. Trefaut-Rodrigues, and Y. Yonenaga-Yasuda. 2007. Chromosomal studies in four species of genus *Chaunus* (Bufonidae, Anura): localization of telomeric and ribosomal sequences after fluorescence in situ hybridization (FISH). Genetica 134:159–168.

Azevedo, M.F.C., F. Foresti, P.R.R. Ramos, and J. Jim. 2003. Comparative cytogenetic studies of *Bufo ictericus*, *B. paracnemis* (Amphibia, Anura) and an intermediate form in sympatry. Genetics and Molecular Biology 26:289–294.

Baldissera Jr., F.A., R.F. Batistic, and C.F.B. Haddad. 1999. Cytotaxonomic considerations with the description of two new NOR locations for South American toads, genus *Bufo* (Anura: Bufonidae). Amphibia-Reptilia 20:413–420.

Baldo, D., and N.G. Basso. 2004. A new species of *Melanophryniscus* Gallardo, 1961 (Anura: Bufonidae), with comments on the species of the genus reported for Misiones, northeastern Argentina. Journal of Herpetology 38:393–403.

Beiswenger, R.E. 1977. Diel patterns of aggregative behavior in tadpoles of *Bufo americanus*, in relation to light and temperature. Ecology 58:98–108.

Breden, F., A. Lum, and R. Wassersug. 1982. Body size and orientation in aggregates of toad tadpoles *Bufo woodhousei*. Copeia 1982:672–680.

Brandão, R.A., N.M. Maciel, and A. Sebben. 2007. A new species of *Chaunus* from central Brazil (Anura; Bufonidae). Journal of Herpetology 41:309–316.

Bogart, J.P. 1968. Chromosome number difference in the Amphibian genus *Bufo*: the *Bufo regularis* species group. Evolution 22:42–45.

Bogart, J.P. 1972. Karyotypes. Pp 171–195 in W.F. Blair (Ed.), Evolution in the Genus *Bufo*. University of Texas Press, USA.

Borteiro, C., F. Kolenc, M. Tedros, and C. Prigioni. 2006. The tadpole of *Chaunus dorbignyi* (Duméril & Bibron) (Anura, Bufonidae). Zootaxa 1308:49–62.

Cadle J.E., and R. Altig. 1991. Two lotic tadpoles from the Andes of Southern Peru: *Hyla armata* and *Bufo veraguensis*, with notes on the call of *Hyla armata* (Amphibia: Anura: Hylidae and Bufonidae). Studies on Neotropical Fauna and Environment 26:45–53.

Caldwell, J.P. 1989. Structure and behaviour of *Hyla geographica* tadpole schools, with comments on classification of group behavior in tadpoles. Copeia 1989:938–948.

Caramaschi, U., and H. Niemeyer. 2003. Nova espécie do complexo de *Bufo margaritifer* (Laurenti, 1768) do estado do Mato Grosso do Sul, Brasil (Amphibia, Anura, Bufonidae). Boletim do Museo Nacional do Rio de Janeiro 501:1–16.

Carr, K.M., and R. Altig. 1991. Oral disc muscles of anuran tadpoles. Journal of Morphology 208:271–277.

Cei, J.M. 1980. Amphibians of Argentina. Monitore Zoologico Italiano Monografia 2: 1–609.

Cunningham, M., and M.I. Cherry. 2004. Molecular systematics of African 20-chromosome toads (Anura: Bufonidae). Molecular Phylogenetics and Evolution 32:671–85.

Echeverría, D.D. 1998. Microanatomía del aparato bucal y de la cavidad oral de la larva de *Bufo fernandezae* Gallardo, 1957 (Anura, Bufonidae), con comentarios acerca de la coloración in vivo y la anatomía externa. Alytes 16:50–60.

Echeverría, D.D., and L.E. Fiorito de López. 1981. Estadios de la metamorfosis en *Bufo arenarum* (Anura). Physis Sección B 40:15–23.

Eluvathingal, L.M., B.A. Shanbhag, and S.K. Saidapur. 2009. Association preference and mechanism of kin recognition in tadpoles of the toad *Bufo melanostictus*. Journal of Bioscience 34:435–444.

Eterovick, P.C. 2000. Efects of aggregation on feeding of *Bufo crucifer* tadpoles (Anura, Bufonidae). Copeia 2000:210–215.

Eterovick, P.C., and I. Sazima. 1999. Description of the tadpole of *Bufo rufus* with notes on aggregative behaviour. Journal of Herpetology 33:711–713.

Fabrezi, M., and R. Vera. 1997. Caracterización morfológica de larvas de anuros del noroeste argentino. Cuadernos de Herpetología 11:37–49.

Fernández, K. 1926. Sobre la biología y reproducción de batracios argentinos Segunda Parte. Boletín de la Academia Nacional de Ciencias de Córdoba 29:271–320.

Fiorito de López, L.E., and D.D. Echeverría. 1989. Microanatomía e histogénesis del aparato bucal en las larvas de *Bufo arenarum* (Anura: Bufonidae). Cuadernos de Herpetología 4:4–10.

Frost, D. R., T. Grant, J. Faivovich, R.H. Bain, A. Haas, C.F.B. Haddad, R.O. De Sá, A. Channing, M. Wilkinson, S.C. Donnellan, C.J. Raxworthy, J.A. Campbell, B.L. Blotto, P. Moler, R.C. Drewes, R.A. Nussbaum, J.D. Lynch, D.M. Green, and W.C. Wheeler. 2006. The Amphibian Tree of Life. Bulletin of the American Museum of Natural History 297:1–370.

Gosner, K.L. 1960. A simplified table for staging anuran embryos and larvae with notes in identification. Herpetologica 16:183–190.

Green, D.M., and S.K. Sessions. 2007. Karyology and cytogenetics. Pp. 2756–2841 in H. Heatwole and M. Tyler (Eds.), Amphibian Biology (Vol. 7). Surrey Beatty and Sons, Australia.

Haas, A. 2003. Phylogeny of frogs as inferred from primarily larval characters (Amphibia: Anura). Cladistics 19:23−89.

Heyer, W.R., A.S. Rand, C.A.G. Da Cruz, O.L. Peixoto, and C.E. Nelson. 1990. Frogs of Boracéia. Arquivos de Zoologia 31:231–410.

Kasahara. S., A.P.Z. Silva, and C.F.B. Haddad. 1996. Chromosome banding in three species of Brazilian toads (Amphibia-Bufonidae). Brazilian Journal of Genetics 19:237–242.

Kenny, J.S. 1969. The amphibia of Trinidad. Studies of the Fauna of Curação and other Caribbean Islands 108:1–78.

Kocher, T.D., W.K. Thomas, A. Meyer, S.V. Edwards, S. Päbo, F.X. Villablanca, and A.C. Wilson. 1989. Dynamics of mitochondrial DNA evolution in animals: amplification and sequencing with conserved primers. Proceedings of the National Academy of Sciences 86:6196–6200.

Kolenc, F., C. Borteiro, D. Baldo, D.P. Ferraro, and C.M. Prigioni. 2009. The tadpoles and advertisement calls of *Pleurodema bibroni* Tschudi and *Pleurodema kriegi* (Müller), with notes on their geographic distribution and conservation status (Amphibia, Anura, Leiuperidae). Zootaxa 1969:1–35.

Kwet, A., M. Di-Bernardo, and R. Maneyro. 2006. First record of *Chaunus achavali* (Anura, Bufonidae) from Rio Grande do Sul, Brazil, with a key for the identification of the species in the *Chaunus marinus* group. Iheringia (Zoologia) 96:479–485.

Lannoo, M.J. 1987. Neuromast topography in anuran amphibians. Journal of Morphology 191:115–129.

Lourenço A.C.C., D. Baêta, A.C.L. Abreu, and J.P. Pombal Jr. 2010. Tadpole and advertisement call of *Rhinella pombali* (Baldissera, Caramaschi & Haddad, 2004) (Amphibia, Anura, Bufonidae). Zootaxa 2370:65–68.

Maciel, N.M., R.A. Brandão, L.A. Campos, and A. Sebben. 2007. A large new species of *Rhinella* (Anura: Bufonidae) from Cerrado of Brazil. Zootaxa 1627:23–39.

Maciel, N.M., R.G. Collevatti, G.R. Colli, and E.F. Schwartz. 2010. Late Miocene diversification and phylogenetic relationships of the huge toads in the *Rhinella marina* (Linnaeus, 1758) species group (Anura: Bufonidae). Molecular Phylogenetics and Evolution 57:787–97.

Maneyro, R., D. Arrieta, and R.O. de Sá. 2004. A new toad (Anura: Bufonidae) from Uruguay. Journal of Herpetology 38:161–165.

Martin, R.F. 1972. Evidence from osteology. Pp. 37–70 in W.F. Blair (Ed.), Evolution in the Genus *Bufo*. University of Texas Press, USA.

McDiarmid, R.W. and R. Altig. 1999. Research. Materials and techniques. Pp. 7–23 in R.W. McDiarmid and R. Altig (Eds.), Tadpoles: The Biology of Anuran Larvae. University of Chicago Press, USA.

Mercês, E.A., F.A. Juncá, and F.S.C. Casal. 2009. Girinos de tres espécies do gênero *Rhinella* Fitzinger, 1826 (Anura-Bufonidae) ocorrentes no Estado da Bahia, Brasil. Sitientibus Série Ciências Biologicas 9:133–138.

Moritz, C., C.J. Schneider, and D.B. Wake. 1992. Evolutionary relationships within the *Ensatina eschscholtzii* complex confirm the ring species interpretation. Systematic Biology 41:273–291.

Rossa-Feres, D. de C., and F. Nomura. 2006. Characterization and taxonomic key for tadpoles (Amphibia: Anura) from the northwestern region of São Paulo State, Brazil. Biota Neotropica 6:1–26.

Savage, J.M. 1960. Geographic variation in the tadpole of the toad, *Bufo marinus*. Copeia 1960:233–236.

Sedra, S. 1950. The metamorphosis of the jaws and their muscles in the toad *Bufo regularis* Reuss, correlated with changes in the animal's feedings habits. Proceedings of the Zoological Society of London 120:405–449.

Stevaux, M.N. 2002. A new species of *Bufo* Laurenti (Anura, Bufonidae) from northeastern Brazil. Revista Brasileira de Zoologia 19:235–242.

Tamura, K., J. Dudley, M. Nei, and S. Kumar. 2007. MEGA4: Molecular Evolutionary Genetics Analysis (MEGA) software version 4.0. Molecular Biology and Evolution 24:1596−1599.

Taylor, W.R., and G.C. Van Dyke. 1985. Revised procedures for staining and clearing small fishes and other vertebrates for bone and cartilage study. Cybium 9:107−119.

Tolledo, J., and L.F. Toledo. 2010. Tadpole of *Rhinella jimi* (Anura: Bufonidae) with comments on the tadpoles of species of the *Rhinella marina* group. Journal of Herpetology 44:480–483.

Tomatis, C., D. Baldo, F. Kolenc, and C. Borteiro. 2009. Chromosomal variation in the species of the *Physalaemus henselii* group (Anura, Leiuperidae). Journal of Herpetology 43:555–560.

Vallinoto, M., F. Sequeira, D. Sodré, J.A.R. Bernardi, I. Sampaio, and H. Schenider. 2010. Phylogeny and biogeography of the *Rhinella marina* species complex (Amphibia, Bufonidae) revisited: implications for Neotropical diversification hypotheses. Zoologica Scripta 39:128–140.

Vera Candioti, M.F. 2007. Anatomy of anuran tadpoles from lentic water bodies: systematic relevance and correlation with feeding habits. Zootaxa 1600:1–175.

Vera Candioti, M.F., and R. Altig. 2010. A survey of shape variation in keratinized labial teeth of anuran larvae as related to phylogeny and ecology. Biological Journal of the Linnean Society 101:609–625.

Vitelli, L., R. Batistoni, F. Andronico, I. Nardi, and G. Barsacchi-Pilone. 1982. Chromosomal localization of 18S + 28S and 5S ribosomal RNA genes in evolutionarily diverse anuran amphibians Chromosoma 84:475–91.

Wassersug, R.J. 1976. Oral morphology of anuran larvae: terminology and general description. Occasional Papers of the Museum of Natural History, University of Kansas 48:1–23.

Wassersug, R.J. 1980. Internal oral features of larvae from eight families: functional, systematic, evolutionary and ecological considerations. Miscelaneous Publications of the Museum of Natural History, University of Kansas 68:1−146.

TABLE 1.— Larval musculature of *Rhinella achavali* at stage 33.

Muscle	Insertions
Mandibulolabialis inferior	ventromedial region of Meckel's cartilage – lower lip of the oral disc
Intermandibularis	medial region of Meckel's cartilage – median aponeurosis
Levator mandibulae longus superficialis	external and posterior margin of the subocular bar – dorsomedial region of Meckel's cartilage
Levator mandibulae longus profundus	external margin of the subocular bar and part of the ascending process of the palatoquadrate – lateroventral margin of the alaof the suprarostral, through a tendon common with that of the m. l.m.e. profundus
Levator mandibulae internus	ventral surface of the ascending process – distal edge of Meckel's cartilage
Levator mandibulae externus superficialis	medial, inferior surface of the muscular process – dorsal, lateral edge of the suprarostral; dorsal to the mandibular branch of the trigeminal nerve (V_3)
Levator mandibulae externus profundus	medial, inferior surface of the muscular process – lateroventral margin of the ala of the suprarostral
Levator mandibulae articularis	inferior part of the medial surface of the

	muscular process – dorsal surface of the lateral edge of Meckel’s cartilage
Levator mandibulae lateralis	dorsal, lateral edge of the suprarostral – articular process of the palatoquadrate
Suspensoriohyoideus	posterior descending margin of the muscular process – posterior surface of the lateral process of the ceratohyal
Orbitohyoideus	anterior, dorsal margin of the muscular process – lateral edge of the ceratohyal
Suspensorioangularis	inferior, lateral part of the descending marginof the muscular process – retroarticular process of Meckel’s cartilage
Quadratoangularis	ventral surface of the palatoquadrate – retroarticular process of Meckel’s cartilage
Hyoangularis	dorsal surface of the ceratohyal, anterior to the articular condyle – retroarticular process of Meckel’s cartilage
Interhyoideus	ventral surface of the ceratohyal, near the lateral edge – median aponeurosis
Geniohyoideus	posterior, ventral surface of the infrarostral – hypobranchial plates, at the level of the ceratobranchial IV
Levator arcuum branchialium I	lateral margin of the subocular bar – ceratobranchial I
Levator arcuum branchialium II	subocular bar – terminal commissure I

Levator arcuum branchialium III	lateroventral part of the otic capsule – terminal commissure II
Levator arcuum branchialium IV + Tympanopharyngeus	the distinction between these two muscles is not clear; from the posterolateral surface of the otic capsule, two slips arise: the lateral slip inserts on the medial margin of the ceratobranchial IV, and the medial slip inserts on the medial margin of the ceratobranchial IV and connective tissue of the pericardium
Dilatator laryngis	posterolateral surface of the otic capsule – arytenoid cartilage
Constrictor branchialis II	branchial process II – terminal commissure I
Constrictor branchialis III	branchial process II – terminal commissure II
Constrictor branchialis IV	branchial process II – distal edge of the ceratobranchial III
Subarcualis rectus I	three slips: lateral base of the posterior process of the ceratohyal – proximal part of the ceratobranchial I (dorsal slip), branchial process II (ventral$_1$ slip), and branchial process III (ventral$_2$ slip)
Subarcualis rectus II-IV	branchial process III, confluent with the ventral$_2$ slip of the m. s. r. I – proximal,

	ventral part of the ceratobranchial IV; a lateral slip inserting distally on the ceratobranchial
Subarcualis obliquus	urobranchial process – branchial process II
Diaphragmatobranchialis	peritoneum – distal edge of the ceratobranchial III
Rectus cervicis	peritoneum – branchial process III
Rectus abdominis	peritoneum – pelvic griddle

TABLE 2.— Morphometric analysis of the chromosomes of *Rhinella achavali*. References: cr, centromeric ratio; ci, centromeric index; m, metacentric; sm, submetacentric; rl, relative length; la, long arm; sa, short arm.

				% of haploid complement		
Pair	cr ± SD	ci ± SD	Type	rl	la	sa
1	1.12±.05	0.47±.01	m	15.97	8.43	7.55
2	1.40±.05	0.42±.01	m	15.43	9.00	6.43
3	1.48±.02	0.41±.01	m	13.35	7.94	5.41
4	1.90±.09	0.35±.01	sm	12.07	7.89	4.17
5	1.20±.11	0.46±.02	m	11.03	6.00	5.04
6	1.22±.13	0.45±.03	m	8.68	4.74	3.95
7	1.36±.14	0.43±.02	m	6.78	3.89	2.89
8	1.28±.20	0.44±.04	m	5.98	3.33	2.65
9	1.31±.09	0.43±.02	m	5.32	3.01	2.31
10	1.36±.20	0.43±.04	m	4.64	2.65	1.99
11	1.32±.16	0.44±.03	m	3.64	2.05	1.60

FIGURE LEGENDS

FIG. 1.— Tadpole of *Rhinella achavali* at stage 31 (MNHN 9470). Lateral view (A), dorsal view (B), and oral disc (C). Scale = 5 mm (A, B) and 1 mm (C).

FIG. 2. — Buccal cavity of *Rhinella achavali* tadpole at stage 33. Buccal roof (A), buccal floor (B), and details of labial teeth (C), choanae (D), and non-colored spurs (E). Scale = 1 mm (A, B) and 10µm (C, D, E).

FIG. 3. — Chondrocranium and hyobranchial skeleton of *Rhinella achavali* tadpole at stage 31. Chondrocranium, dorsal view (A), suprarostral, frontal view (B), lower jaw, frontal view (C), and hyobranchial skeleton, ventral view (D). Scale = 1 mm.

FIG. 4. — Cranial muscles of *Rhinella achavali* tadpole at stage 33. Dorsal (A) and ventral view (B). References: cbII–IV, constrictor branchialis II–IV; db, diaphragmatobranchialis; gh, geniohyoideus; ha, hyoangularis; ih, interhyoideus; im, intermandibularis; labI–IV, levator arcuum branchialium I–IV; lma, levator mandibulae articularis; lmep, levator mandibulae externus profundus; lmes, levator mandibulae externus superficialis; lmi, levator mandibulae internus; lml, levator mandibulae lateralis; lmlp, levator mandibulae longus profundus; lmls,

levator mandibulae longus superficialis; ml, mandibulolabialis; oh, orbitohyoideus; qa, quadratoangularis; rc, rectus cervicis; sa, suspensorioangularis; sh, suspensoriohyoideus; so, subarcualis obliquus; srI–IV, subarcualis rectus I–IV; tp, tympanopharyngeus. Scale = 1 mm.

FIG. 5.— Chromosomes of *Rhinella achavali*. Giemsa stained karyotype (A), C-banded karyotype (B), and Ag-NOR in chromosome pair 7 (inset). Scale = 10 μm.

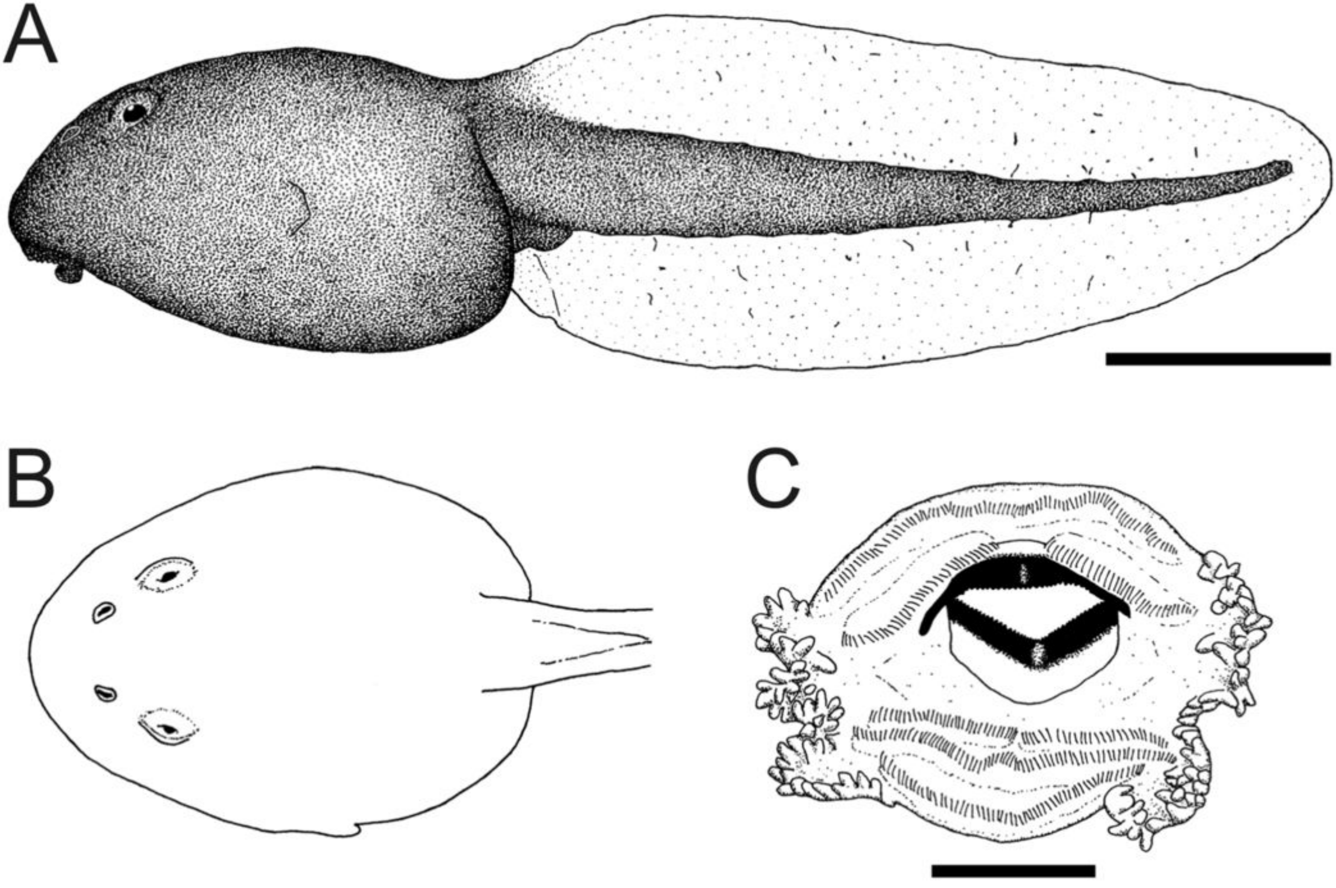
A
B
C

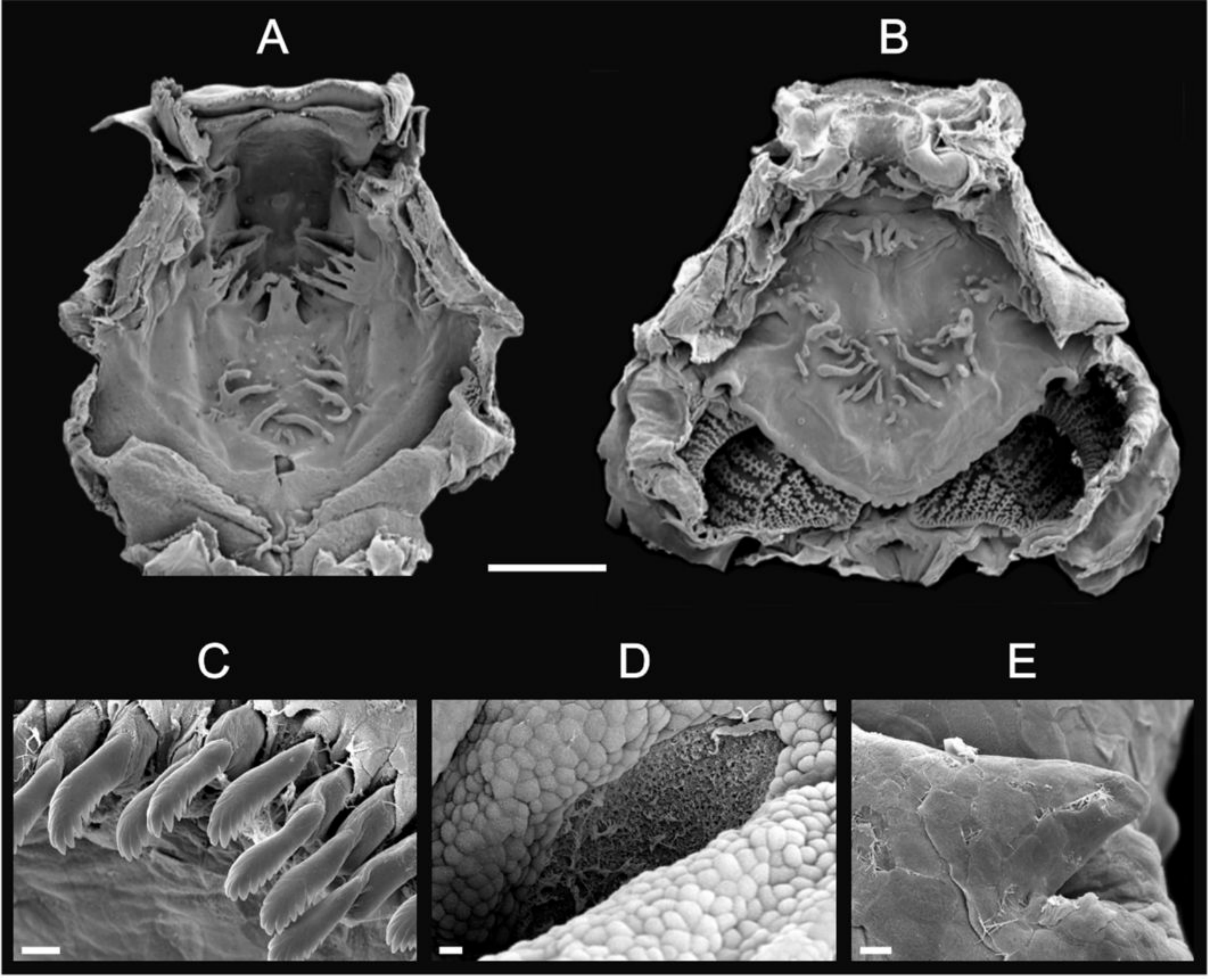

A
B
C
D
E

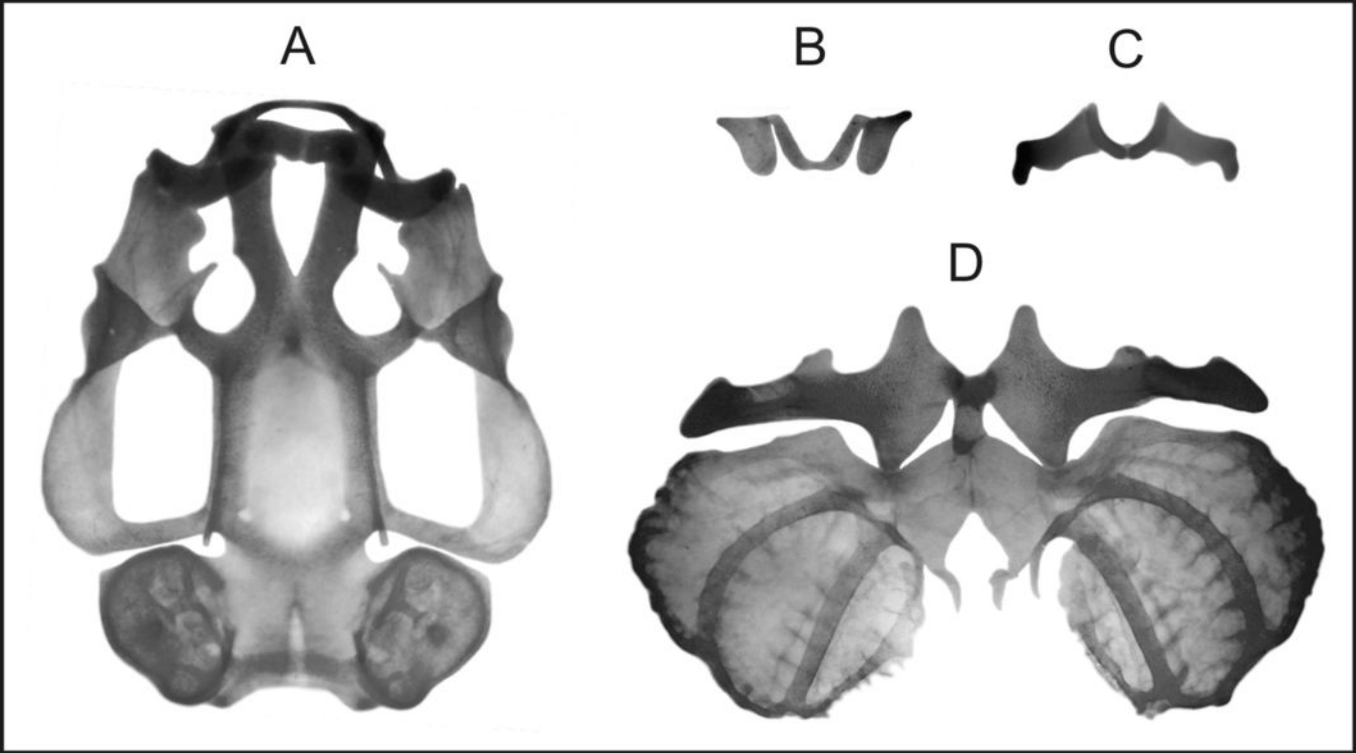
A
B
C
D

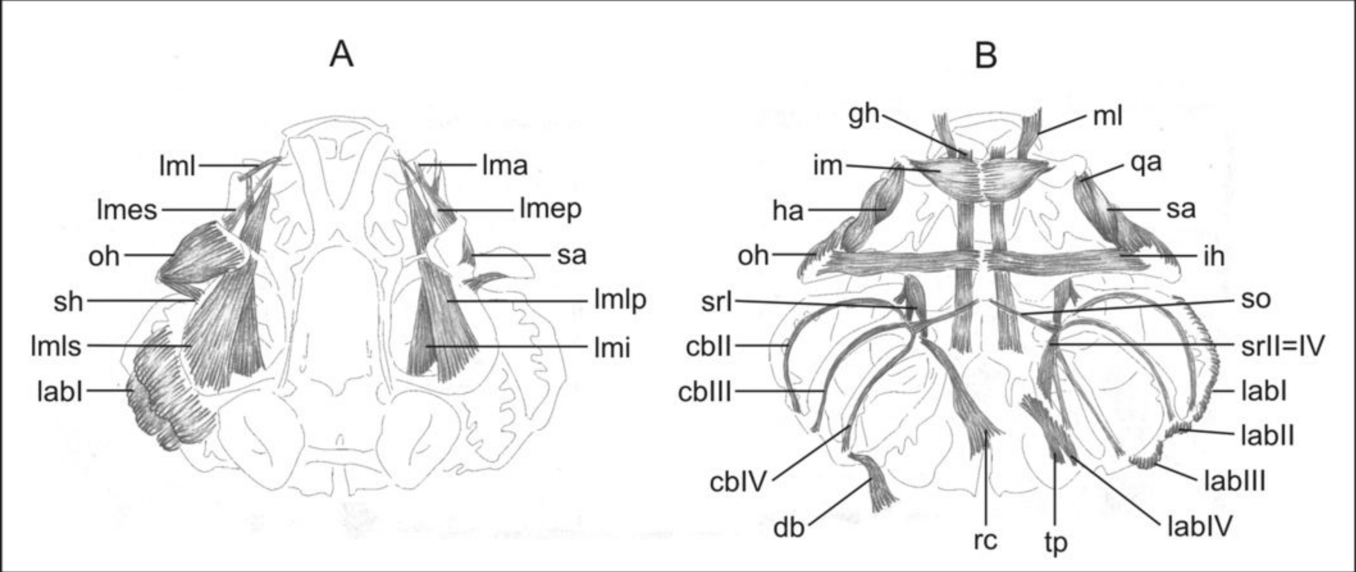

A
B
lml
lma
lmes
lmep
oh
sa
sh
lmlp
lmls
lmi
labI
gh
ml
im
qa
ha
sa
oh
ih
srI
so
cbII
srII=IV
cbIII
labI
labII
cbIV
labIII
db
rc
tp
labIV

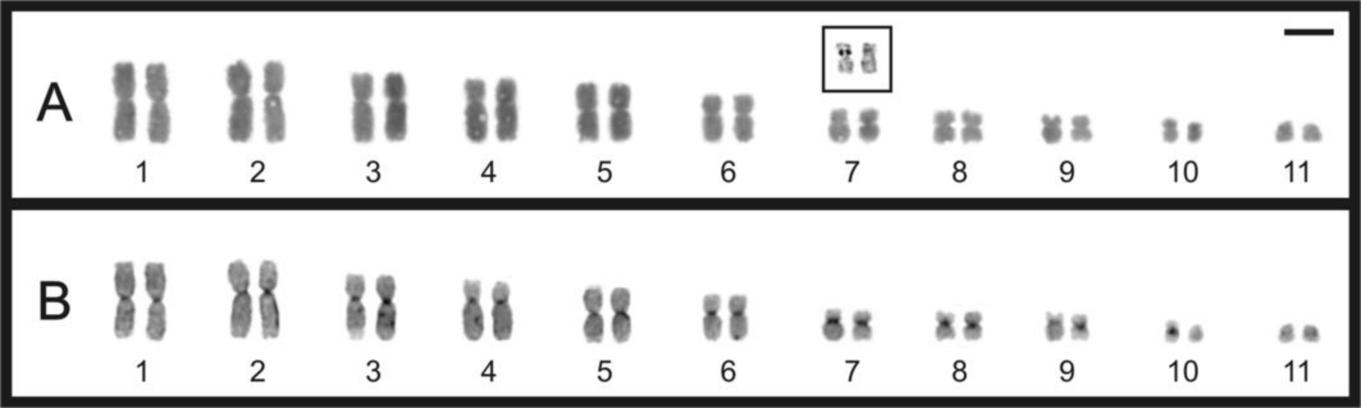
A
1
2
3
4
5
6
7
8
9
10
11
B
1
2
3
4
5
6
7
8
9
10
11